

# X-ray Reflectivity Study of 300 Å Oxidized $\text{Al}_{0.96}\text{Ga}_{0.04}\text{As}$ on a GaAs Substrate

S.-K. Cheong,<sup>1</sup> B. A. Bunker,<sup>1</sup> D. C. Hall,<sup>2</sup> G. L. Snider,<sup>2</sup> P. J. Barrios<sup>2</sup>

<sup>1</sup> Department of Physics, University of Notre Dame, IN, U.S.A.

<sup>2</sup> Department of Electrical Engineering, University of Notre Dame, IN, U.S.A.

## Introduction

Wet-thermal native oxides of AlGaAs<sup>1</sup> have led to numerous advances in optoelectronic devices<sup>2</sup> and have been explored for their potential use in GaAs-based metal-oxide semiconductor (MOS) applications. With a suitable gate oxide, AlGaAs/InGaAs/GaAs-based MOSFET devices could significantly outperform present Si electronics due to lower effective mass, higher electron mobility, and higher saturated velocity. In producing these insulating layers, however, the structure of the oxide and the nature of the interface are not well understood. The goal of this study is to correlate the physical structure to electronic properties and sample preparation methods.

X-ray specular reflectivity is a powerful nondestructive technique to investigate the bulk properties, such as the density profile as a function of depth, thickness of oxide layer and roughness of both surface and interface.

## Materials and Methods

A thin 300 Å  $\text{Al}_{0.94}\text{Ga}_{0.06}\text{As}$  film on a GaAs substrate is surface oxidized using the methods described previously.<sup>3</sup> To investigate the density profile as a function of depth, x-ray specular reflectivity is measured at the MRCAT 10-ID line using an 8-circle Huber diffractometer.

The x-ray energy is tuned at 300 eV above the Ga K-edge (10667 eV; x-ray wavelength = 1.1623 Å), and the dimension of the incident beam size is defined as approximately 50 μm horizontal width by 3 mm with two slits. We also use two slits after the sample to reduce the background scattering and assure that all the beam reflected off the sample is detected—the slit dimensions were 500 μm × 5 mm for the first and 800 μm × 5 mm for the second slit.

## Results

For reflectivity analysis we use the model-independent methods,<sup>4</sup> i.e., without assuming *a priori* distribution of electron density profile across the film, based on the distorted wave Born approximation (DWBA).<sup>5</sup> The general approach is as follows. We fix the average electron density ( $\rho_0$ ), thickness ( $d$ ) of the film, and the roughness of surface ( $\sigma_1$ ) and interface ( $\sigma_2$ ) at the best value obtained by assuming a uniform density film. The following are the best-fit values from the one-layer model (uniform density model):  $\rho_0=1.244 \text{ \AA}^{-3}$ ,  $d=262.0\pm 1.5 \text{ \AA}$ ,  $\sigma_1=5.3\pm 0.5 \text{ \AA}$ , and  $\sigma_2=5.0\pm 0.5 \text{ \AA}$ .

The film is then divided into a series of constant electron density slabs of density  $\rho_0(z_i) + \Delta\rho(z_i)$ . Each slab has a width of  $\pi/q_{max}$ , where  $q_{max}$  is the highest  $q_z$  reached by the reflectivity scan. The values of  $\Delta\rho(z_i)$  in each slab are then varied until the best fit to the data is obtained. For this sample 40 slabs with 7 Å thickness each are used to describe a region up to 280 Å deep from the surface.

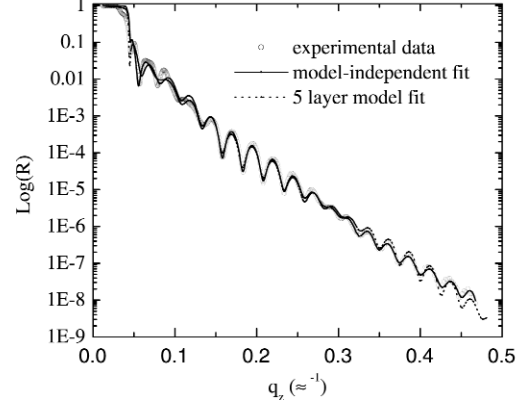


FIG. 1. The measured x-ray reflectivity data of 300 Å oxidized  $\text{Al}_{0.94}\text{Ga}_{0.06}\text{As}$  on GaAs (open circles); best fit using a model-independent method (solid line); best fit using a Parratt's method (dotted line).

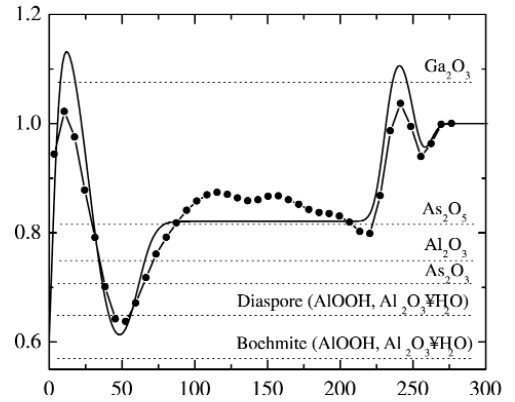


FIG. 2. Calculated electron density profile from the model-independent fit (solid lines with symbols); from the Parratt's method (solid line); electron densities of several reference compounds (dotted line).

The resulting best fit from model-independent methods is shown in Fig. 1 as a solid line through the data, and the resulting density profile is shown in Fig. 2 as a solid line with symbols along with several reference bulk densities.

The data are also analyzed using conventional Parratt's formalism,<sup>6</sup> i.e., assuming a model based on the model-independent fit results and floating parameters, such as electron density, thickness, and roughness of each layer. The best fit is obtained by five sublayers on a GaAs substrate, as shown in Fig. 1 as a dotted line, and the resulting density profile is shown in Fig. 2 as a solid line. The detailed structural parameters derived by this simulation are summarized in Table I.

## Discussion

From the fit results using both model-independent method and Parratt's method described as the above, a high electron density layer (~25 Å) exists at the surface with a density very close

TABLE I. Values of parameters deduced from the calculation using Parratt's method.  $L_i$  ( $i=1, 2, \dots, 5$ ) correspond to sublayers from the surface on a GaAs substrate.  $\rho$  represents an average electron density of each sublayer; the electron density of GaAs ( $\rho_{\text{GaAs}} = 1.414 \text{ \AA}^{-3}$  ( $=5.31 \text{ g/cm}^3$ )).

Layer	Thickness ( $\text{\AA}$ )	Roughness ( $\text{\AA}$ )	$\rho/\rho_{\text{GaAs}}$
$L_1$	27.1 $\pm$ 1.5	5.7 $\pm$ 0.5	1.22 $\pm$ 0.1
$L_2$	33.6 $\pm$ 1.5	11.8 $\pm$ 0.5	0.57 $\pm$ 0.1
$L_3$	169.6 $\pm$ 1.5	9.0 $\pm$ 0.5	0.82 $\pm$ 0.1
$L_4$	19.5 $\pm$ 1.5	5.9 $\pm$ 0.5	1.13 $\pm$ 0.1
$L_5$	11.9 $\pm$ 1.5	6.1 $\pm$ 0.5	0.92 $\pm$ 0.1
GaAs	—	4.6 $\pm$ 0.5	1.0

to that of GaAs, as can be seen in Fig. 2 and Table I, suggesting that the presence of a thin oxidized GaAs surface layer may be attributed to a residue of the original 500  $\text{\AA}$  GaAs protective cap not fully removed by a citric acid/hydrogen peroxide selective etch before oxidation. The presence of GaAs at the surface is confirmed by reflection-mode XAFS.<sup>7</sup> A low-density layer ( $\sim 30 \text{ \AA}$ ) overlying a higher density oxide layer (170  $\text{\AA}$ ) is possibly due to the formation of lower density Al hydroxides than in the deeper layer.

## Acknowledgments

This work was supported in part by Air Force Office of Scientific Research Grant F49620-98-1-0120. The MRCAT is sup-

ported by the U. S. Department of Energy (DoE) under Contract DE-FG02-94-ER45525 and the member institutions. Use of the APS was supported by the U.S. DOE, under Contract No. W-31-109-Eng-38.

## References

- <sup>1</sup> J.M. Dallesasse, N. Holonyak, Jr., A.R. Sugg, T.A. Richard, and N. El-Zein, Appl. Phys. Lett. **57**, 2844 (1990).
- <sup>2</sup> K.D. Choquette, K.M. Geib, C.I.H. Ashby, R.D. Twisten, O. Blum, H.Q. Hou, D.M. Follstaedt, B.E. Hammons, D. Mathes, and R. Hull, IEEE J. Sel. Top. Quantum Electron. **3**, 916 (1997).
- <sup>3</sup> C.B. DeMelo, D.C. Hall, G.L. Snider, D. Xu, G. Kramer, and N. El-Zein, Electron. Lett. **36**, 84 (2000) and references therein.
- <sup>4</sup> M K. Sanyal, J.K. Basu, A. Datta, and S. Banerjee, Europhys. Lett. **36**, 265 (1996).
- <sup>5</sup> S.K. Sinha, E.B. Sirota, S. Garoff, and H.B. Stanley, Phys. Rev. B **38**, 2297 (1988).
- <sup>6</sup> L.G. Parratt, Phys. Rev. **95**, 359 (1954)
- <sup>7</sup> S.-K. Cheong, B.A. Bunker, D.C. Hall, G.L. Snider, and P.J. Barrios, in Argonne National Laboratory Report ANL-01/03.